Differences in innate immune cell populations distinguish autoimmune from herpesvirus-associated encephalitis

Saskia Räuber, Andreas Schulte-Mecklenbeck, Kelvin Sarink, Kristin S. Golombeck, Christina B. Schroeter, Alice Willison, Christopher Nelke, Christine Strippel, Andre Dik, Marco Gallus, Stjepana Kovac, Heinz Wiendl, Gerd Meyer zu Hörste, Tobias Ruck, Oliver M. Grauer, Udo Dannlowski, Tim Hahn, Catharina C. Gross, Sven G. Meuth, Nico Melzer

Journal of Autoimmunity 152 (2025) 103396

Contents lists available at ScienceDirect

Journal of Autoimmunity

journal homepage: www.elsevier.com/locate/jautimm

Differences in innate immune cell populations distinguish autoimmune from herpesvirus-associated encephalitis

Saskia Räuber [a,b], Andreas Schulte-Mecklenbeck [a], Kelvin Sarink [c], Kristin S. Golombeck [a], Christina B. Schroeter [a,b], Alice Willison [b], Christopher Nelke [a], Christine Strippel [a], Andre Dik [a], Marco Gallus [a], Stjepana Kovac [a], Heinz Wiendl [a], Gerd Meyer zu Hörste [a], Tobias Ruck [a,b], Oliver M. Grauer [a], Udo Dannlowski [c], Tim Hahn [c], Catharina C. Gross [a], Sven G. Meuth [a,b,1], Nico Melzer [a,b,1,*]

[a] Department of Neurology with Institute of Translational Neurology, University of Münster, Münster, Germany
[b] Department of Neurology, Medical Faculty and University Hospital Düsseldorf, Heinrich Heine University Düsseldorf, Düsseldorf, Germany
[c] Institute for Translational Psychiatry, University of Münster, Münster, Germany

ARTICLE INFO

Handling Editor: Professor C Selmi

Keywords:
Autoimmune encephalitis
Multidimensional flow cytometry
Immune cells
Herpes virus infections
Differential diagnoses

ABSTRACT

Background: Autoimmune encephalitis (AIE) is a disabling inflammatory condition of the brain deemed to be due to a dysregulated immune response. Viral infections and malignancies together with certain genetic polymorphisms are thought to contribute to the pathogenesis of AIE, yet the exact mechanisms remain insufficiently understood. Diagnosis of AIE currently relies on clinical consensus criteria. However, diagnostic workup can be challenging in some cases, potentially delaying treatment initiation associated with poor clinical outcomes.
This study aims to investigate the systemic and intrathecal immune cell profiles of AIE in comparison to viral meningoencephalitis (VME) as a clinically relevant differential diagnosis and evaluate its diagnostic and therapeutic potential.
Methods: 97 mainly treatment-naïve AIE patients, 47 patients with VME, and 109 somatic symptom disorder (SD) controls were included. Analysis of peripheral blood (PB) and cerebrospinal fluid (CSF) immune cell profiles was performed using multidimensional flow cytometry (mFC) in combination with novel computational approaches.
Results: We were able to identify alterations in the adaptive B and T cell-mediated immune response in AIE compared to SD controls which correspond to respective changes in the brain parenchyma. AIE and VME exhibit similar patterns of adaptive B and T cell responses and differ in pattern of innate immunity especially NK cells. MFC together with routine CSF parameters can differentiate AIE from VME and SD controls implying diagnostic potential.
Conclusion: AIE is characterized by a B and T cell-mediated systemic and intrathecal immune-cell signature which corresponds to changes reported in the brain parenchyma providing insights into immunopathogenesis. Differences between AIE and VME were most prominent for the innate immune response indicating a potential role of NK cells in the pathogenesis of autoimmunity. Our data provides evidence that mFC could be a novel complementary approach to the diagnosis of AIE with diagnostic, therapeutic, and prognostic implications.

1. Introduction

Autoimmune encephalitis (AIE) is an inflammatory condition of the brain, predominantly affecting the grey matter of the central nervous system (CNS) [1,2]. It is a major cause of encephalitis alongside infectious encephalitis and acute disseminated encephalomyelitis (ADEM) [3,4]. The most common form of AIE is anti-N-methyl-D-aspartate receptor encephalitis (NMDARE), typically presenting with psychiatric symptoms, memory disturbance, seizures, movement disorders, language deficits, reduced level of consciousness, and autonomic instability [5,6]. Another typical clinical presentation of AIE is autoimmune limbic encephalitis (ALE). A variety of autoantibodies can be detected in serum

* Corresponding author. Department of Neurology University Hospital Düsseldorf Moorenstraße 5, Bldg. 13.53, Düsseldorf, Germany.
E-mail address: Nico.Melzer@med.uni-duesseldorf.de (N. Melzer).
[1] These authors contributed equally.

https://doi.org/10.1016/j.jaut.2025.103396
Received 29 August 2024; Received in revised form 26 February 2025; Accepted 28 February 2025
Available online 4 March 2025

and/or cerebrospinal fluid (CSF) of patients with ALE (referred to as antibody-positive ALE), first and foremost those against leucine-rich, glioma inactivated 1 (LGI1) and the 65 kDa isoform of the glutamic acid decarboxylase (GAD65). ALE is clinically characterized by temporal lobe seizures, behavioral changes, and memory deficits [1,2].

Diagnostic criteria for AIE in children and adults have been suggested, comprising clinical presentation and results of technical studies (e.g. electroencephalography (EEG), magnetic resonance imaging (MRI), and CSF analysis) [5,7]. Detection of autoantibodies in serum and or CSF together with typical clinical symptoms can support the diagnosis of AIE [5]. However, the clinical diagnosis can be challenging in some cases, especially in patients without detectable autoantibodies in serum or CSF (referred to as antibody-negative ALE (AAB^{-}ALE)), delaying initiation of immunotherapy associated with worse outcomes [8,9].

Technical and conceptual advances over the last years facilitated a more precise clinical and pathophysiological characterization of AIE and led to an increasing number of detectable autoantibodies in serum or CSF [10,11]. Apart from the pathophysiological role of autoantibodies, previous studies support the relevance of immune cells in the pathogenesis of AIE. Differences in the relative contribution of adaptive immune effector mechanisms within the brain parenchyma were apparently based on the cellular localization of the respective target antigens [11–13]. In AIE with autoantibodies against surface membrane neural antigens (e.g. NMDAR, LGI1), autoantibodies have been shown to disrupt epitope function, cross-link targeted antigens, with subsequent internalization of the antibody-antigen complex, activate complement, and instigate cytotoxicity depending on the immunoglobulin subclass [14,15]. However, recent findings also suggest a role for neural-antigen specific cytotoxic T cells in this group of AIE syndromes [16,17].

In AIE with autoantibodies against intracellular neural antigens (e.g. Hu, GAD65), autoantibodies are considered non-pathogenic except for those binding to antigens transiently exposed to the surface membrane e.g. during vesicle exo- and endocytosis [16,18,19]. In this group of AIE syndromes, neural-antigen specific cytotoxic T cells are thought to interact with the cells expressing the target antigen resulting in release of cytokines and different cytotoxic effector molecules that mediate cell dysfunction and destruction [14,17,20,21].

Different factors were linked to the immunopathogenesis of AIE (reviewed in Refs. [22,23]): (i) there seems to be a rather strong genetic predisposition in many AIE syndromes comprising associations inside and also outside the human leukocyte antigen (HLA) locus; (ii) various malignancies expressing neural or structurally related antigens and (iii) systemic and cerebral viral infections together with (iv) defective immune regulatory mechanisms may cause break-down of immune tolerance and promote AIE [22,24,25].

Multidimensional flow cytometry (mFC) is a powerful tool to perform broad characterization of local immune cell composition [26,27]. It can provide insights into the immune effector mechanisms contributing to the pathogenesis of AIE and identify immune cell signatures distinguishing AIE from clinical differential diagnoses. A recently published study assessed the differences in the immune cell profile between patients with NMDARE and VME and reported increased neutrophil counts and a higher monocyte-to-lymphocyte ratio in the PB of NMDARE patients in relation to VME and controls. In the CSF, T lymphocytes, especially $CD4^{+}$ T cells were decreased in NMDARE compared to VME. Higher percentages of $CD8^{+}$ T cells in PB and CSF correlated with disease severity of NMDARE [28]. Even though the study provides first insights into the immunological differences between NMDARE and VME, the study features several limitations, e.g., only lymphocyte subsets were analyzed by mFC, no patients with other subtypes of AIE were included, and the control cohorts were insufficiently characterized.

Applying mFC combined with novel computational approaches, we here provide a detailed characterization of the peripheral and intrathecal immune cell profile of mainly immunotherapy-naïve patients with a more generalized AIE (i.e. NMDARE) and more focal AIE (i.e. ALE with and without different autoantibodies) and compare them to acute VME (aVME) and post-acute VME (pVME) as relevant clinical differential diagnoses, and non-inflammatory controls.

We aimed to enhance the understanding of the immunopathogenesis of AIE and evaluate the benefit of mFC as a complementary tool to the diagnostic workup of AIE facilitating early diagnosis and treatment to improve clinical outcomes.

2. Methods

2.1. Retrospective identification of patients

We retrospectively searched the clinical database of the Department of Neurology at the University Hospital Münster, Germany, to identify immunotherapy-naïve patients diagnosed with NMDARE and ALE with and without different autoantibodies according to the diagnostic criteria suggested by Graus et al. [5] who received mFC of PB and CSF. Detection of neural autoantibodies in serum and/or CSF was performed using a combination of tissue- and cell-based immunofluorescence assays and immunoblotting by the Clinical Immunological Laboratory Prof. h.c. (RCH) Dr. med. Winfried Stöcker, Groβ Grönau (Germany). The following antibodies were assessed: Hu, Ri, ANNA-3, Yo, Tr/DNER, Myelin, Ma/Ta, GAD65, Amphiphysin, Aquaporin-4, NMDA receptor, AMPA receptor, GABA-A/B receptor, LGI1, CASPR2, ZIC4, DPPX, glycine receptor, mGluR1, mGluR5, Rho-GTPase activating protein 26, ITPR1, Homer 3, MOG, Neurochondrin, GluRD2, Flotillin 1/2, IgLON5, CV2, Recoverin, SOX1, Titin, VGKC, Neurexin-3α, GFAP. ALE and NMDARE patients together are referred to as AIE.

Patients with VME were enrolled if herpes viruses (herpes simplex virus 1/2 [HSV], Epstein-Barr virus [EBV], or varicella-zoster virus [VZV]) could be detected in the CSF by polymerase chain reaction (PCR). Patients with VME showed typical clinical signs of encephalitis (e.g. headaches, fever, altered mental status, seizures, psychiatric symptoms, focal neurological abnormalities). Routine CSF studies were compatible with VME, and diagnosis was made based on the detection of virus DNA (HSV, VZV, or EBV) by PCR of CSF. VME was classified as acute, if virus DNA could be detected in the CSF sample at the time of mFC analysis. Post-acute VME was assumed if virus DNA could no longer be detected in the CSF sample at time of mFC analysis (mean time between positive PCR and mFC sample taking: 13.31 ± 9.61 days). Patients with somatic symptom disorder (SD; F45.0 or F45.1), diagnosed according to the ICD-10 diagnostic criteria [29,30], served as non-inflammatory controls (referred to as SD controls (SD)). SD controls had no comorbid neurological conditions. All SD subjects exhibited intrathecal leukocyte counts of <5 cells/μl, intrathecal lactate levels <2 mmol/l, an intact blood-CSF barrier (BCSFB) as indicated by the age-adjusted albumin ratio (QAlb), no intrathecal immunoglobulin synthesis according to Reiber criteria, and an oligoclonal band (ocb) pattern type 1 as described previously [27,31]. Patients with comorbid systemic autoimmune disease, chronic infections or patients treated with immunosuppressants (except for steroids) prior to sampling were excluded from our study. The NMDARE, ALE and SD cohorts were used before [27,31–33].

All patients have been admitted to the Department of Neurology of the University Hospital Münster, Germany, since 2011 and received mFC of PB and CSF during routine clinical workup. Data were anonymized and analysis was performed retrospectively. The study was performed according to the Declaration of Helsinki and was approved by the local Ethics Committee of the Board of Physicians of the Region Westfalen-Lippe and of the University of Münster, Germany (reference number: 2019-712-f-S). All patients provided written informed consent to participate in the study.

2.2. Routine CSF analysis

Lumbar puncture was performed during the clinical routine workup

and samples were processed within 1 h. A Fuchs-Rosenthal chamber was used to assess CSF white blood cell counts (WBC). Protein/albumin concentration and immunoglobulin levels (IgG, IgA, and IgM) were measured by nephelometry. In order to evaluate the integrity of the blood-CSF-barrier, serum and CSF albumin, and immunoglobulin concentrations were compared and a Reiber scheme was created [34]. Ocbs were detected by isoelectric focusing and silver nitrate staining.

2.3. Multidimensional flow cytometry (mFC)

MFC of PB and CSF was performed as part of the routine workup at our center during normal working hours. Fresh PB and CSF samples were used for multidimensional flow cytometry, which is an accredited method. The minimum sample volume was 3 mL. All samples were processed within 1 h of sampling. The flow cytometer was checked by Flow-Check Fluorospheres (Beckman Coulter) on a daily basis. IMMUNO-TROL cells (Beckman Coulter) were used as reference control to ensure validity of the results. CSF samples were centrifuged at 300×*g* for 15 min. Supernatant was discarded and CSF cells were resuspended in parallel to 100 µl PB in 100 µl VersaLyse. Samples were stained based on an established protocol using the antibodies listed in Table 1 [35]. A Navios® flow cytometer (Beckmann Coulter) and the software Kaluza® (version 2.1) were used for data analysis. Paired PB and CSF samples were analyzed and gates were set by comparing CSF with PB samples ensuring a reliable identification of even small cell populations. Gating was performed as described previously [27]. First, leukocytes were identified as CD45 positive cells. Next, leukocyte subsets were separated into granulocytes (Granulo; SSC^{high}CD14-), monocytes (Mono; SSC^{int}CD14+), and lymphocytes (Lympho; SSC^{low}CD14-). Lymphocytes were further divided into B cells (Bc; $CD19^{high}$CD138-), plasma cells (Pc; $CD19^{low}CD138^{high}$), and T cells (Tc; CD3+CD56-). T cells were further classified into $CD4^+$ T cells (CD4+CD8-), $CD8^+$ T cells (CD4-CD8+), and $CD4^+CD8^+$ T cells (CD4+CD8+). Furthermore, expression of the activation marker HLA-DR was analyzed on $CD4^+$ T cells (CD4+HLADR+) and $CD8^+$ T cells (CD8+HLADR+). Natural killer cells (NK) cells were selected as CD56+CD3- cells and were subdivided into $CD56^{bright}$ NK cells (NK bright; $CD56^{bright}CD16^{dim/-}$) and $CD56^{dim}$ NK cells (NK dim; $CD56^{dim}$CD16+). Natural killer T cells (NKT) were identified as CD56+CD3+ cells. Moreover, monocyte subsets were selected as cMono ($CD14^{high}$CD16-), iMono (CD14+ CD16+), and ncMono ($CD14^{low}CD16^{high}$) cells. Percentages of either PB or CSF immune cell populations were compared between groups.

2.4. Data analysis

MFC data acquired during clinical routine workup were retrospectively analyzed using GraphPad Prism (version 9.0.0) and R studio (v1.3.1093). UMAPs (uniform manifold approximation and projection for dimension reduction) were created with the R packages 'umap' (v0.2.10.0) and 'ggplot2' (v3.4.4). Data were scaled and centered in advance. Heatmaps were created using the R package 'pheatmap' (v1.0.12). The group medians for each parameter were calculated and data were scaled row wise. Violin plots were created with the R package 'ggplot2' (v3.4.4). P-values were calculated using Kruskal Wallis test with Dunn post hoc test (p-adjustment method: Benjamini–Hochberg) as normality could not be assumed based on Shapiro–Wilk test. For binary data, Fisher's exact test was used. A p-value ≤ 0.05 was considered statistically significant. Multiple linear regression was performed to adjust for differences in age and sex between groups (CSF/PB parameters as dependent variables, age, sex, and group as independent variables). Sparse Partial Least Squares Discriminant Analysis (sPLS-DA) was applied to evaluate the performance of the PB mFC parameters, the CSF routine parameters, and the combination of CSF routine with PB/CSF mFC parameters to differentiate between groups. SPLS-DA was performed using the R package 'mixOmics' (v6.26.0). The 'auroc' function was used to calculate the Area Under the Curve (AUC) for the classification results obtained from sPLS-DA, higher values indicating better performance. In addition, the contribution of the top ten variables on latent component 1 was visualized.

Table 1
Antibodies for mFC analysis.

Antibodies (Clone)	Company	Identifier
CD3 (UCHT1)	Beckman Coulter	#A66327
CD4 (13B8.2)	Beckman Coulter	#IM2468
CD8 (B9.11)	Beckman Coulter	#A82791
CD14 (RM052)	Beckman Coulter	#B36297
CD16 (3G8)	Beckman Coulter	#A66330
CD19 (J3-119)	Beckman Coulter	#B76283
CD45 (J33)	Beckman Coulter	#B36294
CD56 (N901)	Beckman Coulter	#A21692
CD138 (B-A38)	Beckman Coulter	#A40316
HLA-DR (Immu-357)	Beckman Coulter	#B92438

mFC - multidimensional flow cytometry.

3. Results

3.1. Basic cohort characteristics

In total, 253 patients were enrolled (17 NMDARE, 80 ALE, 47 VME, and 109 SD). The study design is illustrated in Fig. 1A. 62.5 % of ALE patients met the diagnosis of definite ALE, 33.75 % of possible ALE, and 3.75 % of probable ALE according to Graus et al. (Fig. 1A–Supplementary Table 1) [5]. All NMDARE patients fulfilled the criteria of definite NMDARE (Supplementary Table 1) [5]. 26.3 % of ALE patients had antibodies against extracellular target antigens (LGI1 = 11, CASPR2 = 3, GABA-B-R = 2, GABA-A-R = 1, DPPX = 2, VGKC = 1, Neurexin-3α = 1 patient(s)), 21.3 % against intracellular target antigens (GAD65 = 11, Hu = 2, Ma/Ta = 2, Yo, Ma/Ta = 1, Hu/Sox/ZIC4/Yo = 1 patient(s)), 50.0 % were antibody-negative, and two patients had antibodies targeting an unknown antigen. Detailed clinical characteristics of AIE patients are summarized in Supplementary Table 1. None of the patients were receiving immunotherapy at the time of mFC analysis. 19 AIE patients had received steroids at any time point prior to sampling (19.4 %), and one patient plasmapheresis (1.0 %). None of the patients were treated with other immunosuppressants (e.g. rituximab, azathioprine, cyclophosphamide, or methotrexate) before. Mean age was similar between ALE and VME patients (ALE: 55.1 ± 14.5, aVME: 50.7 ± 21.3, pVME: 53.1 ± 18.3 years) while NMDARE patients and SD subjects were younger on average (NMDARE: 39.8 ± 20.4, SD: 39.8 ± 16.9 years). Sex was slightly imbalanced towards male in the ALE and VME group (% female: 42.5 [ALE], 36.8 [aVME], 43.9 [pVME]) while a female predominance was noted for the NMDARE and SD group (% female: 70.6 [NMDARE] and 69.1 [SD]).

3.2. ALE, NMDARE, and VME patients feature elevated CSF WBC, an impaired blood-CSF-barrier, and intrathecal immunoglobulin synthesis

Comparison of CSF routine parameters between groups revealed elevated CSF white blood cell counts in ALE, NMDARE, aVME, and pVME patients compared to SD controls. CSF white blood cell count was highest in aVME, followed by pVME, NMDARE, and then by ALE patients (Fig. 1B). CSF protein levels were elevated in ALE, aVME, and pVME patients in relation to SD controls, with the highest levels seen in patients with aVME (Fig. 1C). More patients with ALE, NMDARE, aVME, and pVME had an impaired blood-CSF-barrier with an increased QAlb compared to SD controls. QAlb was highest in aVME, followed by pVME, ALE, and finally NMDARE patients (Fig. 1D and E). The percentage of patients with intrathecal immunoglobulin synthesis and CSF oligoclonal bands was higher in ALE, NMDARE, aVME, and pVME than in SD controls. NMDARE, aVME, and pVME patients showed more often intrathecal immunoglobulin synthesis and/or CSF oligoclonal bands than

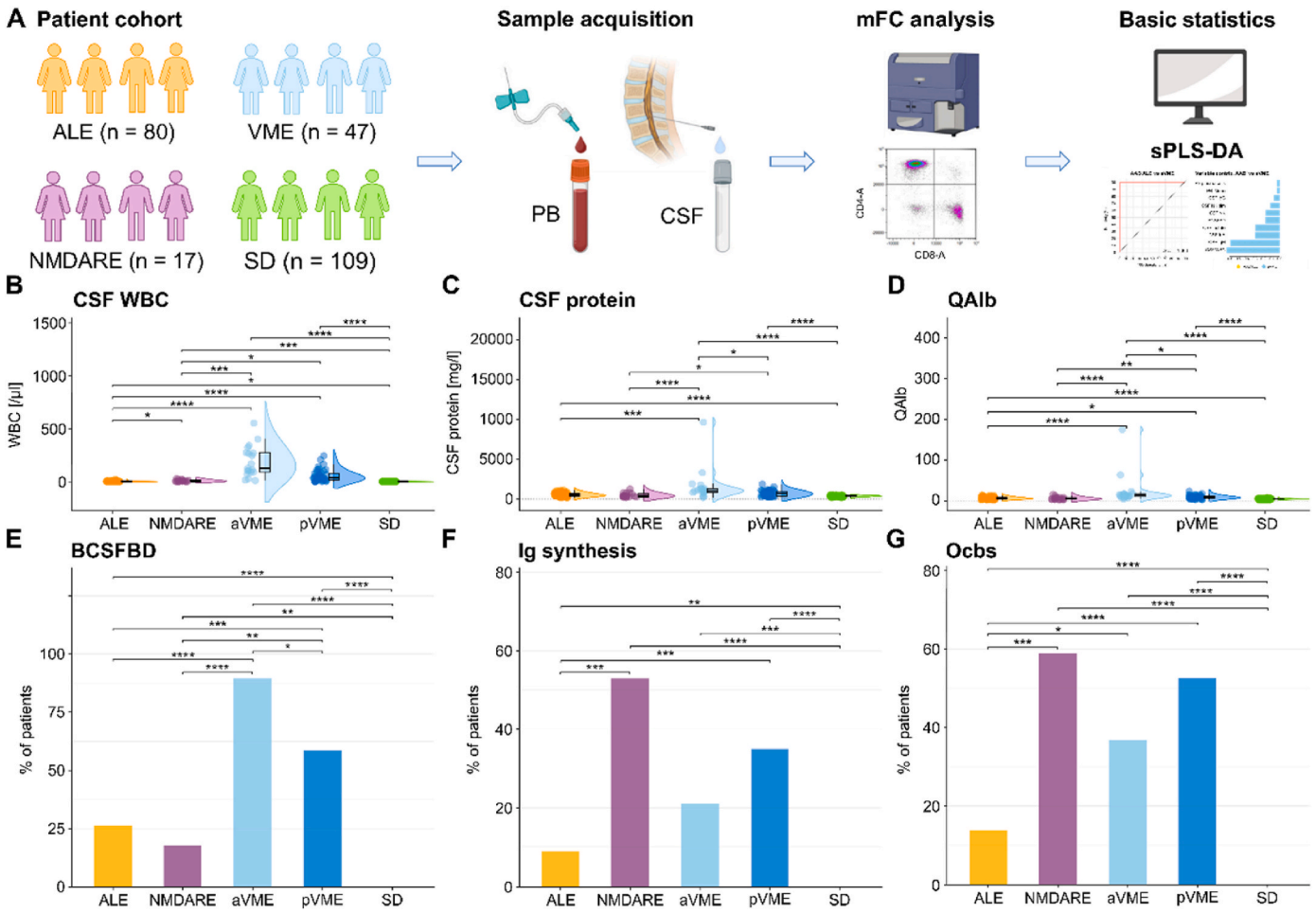

Fig. 1. Basic demographics and clinical parameters of ALE, NMDARE, and VME patients.
A Study design, created in BioRender. Räuber, S. (2024) https://BioRender.com/l54t980: The ALE cohort was further subdivided into ALE patients with autoantibodies against extracellular target antigens (ALE-Extra, 26.3 %), ALE patients with autoantibodies against intracellular target antigens (ALE-Intra, 21.3 %), and ALE patients without autoantibodies (AAB$^-$ ALE, 50.0 %). Two patients had autoantibodies targeting an unknown antigen. VME was classified as acute (aVME, 31.67 %), if virus DNA could be detected in the CSF sample at the time of mFC analysis. Post-acute VME (pVME, 68.33 %) was assumed if virus DNA could no longer be detected in the CSF sample at time of mFC analysis; **B-G** Violin plots with overlaying boxplots and bar plots illustrating the routine CSF parameters. Boxes display the median as well as the 25th and 75th percentiles. The whiskers extend from the hinge to the largest and smallest values, respectively, but no further than 1.5 * IQR from the hinge. Significance was assessed using Kruskal Wallis test with Dunn post hoc test (p-adjustment method: Benjamini–Hochberg) as normality could not be assumed based on Shapiro–Wilk test. For binary data, Fisher's exact test was used.
A - Area; ALE - autoimmune limbic encephalitis; aVME - acute viral meningoencephalitis; BCSFBD - blood-CSF barrier dysfunction; CSF - cerebrospinal fluid; Ig - immunoglobulin; mFC - multidimensional flow cytometry; NMDARE - anti-N-methyl-D-aspartate receptor encephalitis; ocbs - oligoclonal bands; PB - peripheral blood; pVME - post-acute viral meningoencephalitis; QAlb - CSF/serum albumin ratio; VME - viral meningoencephalitis; SD - somatic symptom disorder; sPLS-DA - Sparse Partial Least Squares Discriminant Analysis; WBC - white blood cell count.
** p-value ≤ 0.05; ** p-value ≤ 0.01; *** p-value ≤ 0.001; **** p-value ≤ 0.0001.*

ALE patients (Fig. 1F and G).

In summary, ALE, NMDARE, aVME, and pVME patients share an elevated CSF white blood cell count, an impaired blood-CSF-barrier, and higher probability of intrathecal immunoglobulin synthesis, and CSF oligoclonal band detection.

3.3. Pronounced intrathecal B and plasma cell response in ALE with AABs and increased T cell response in AAB$^-$ ALE

We first assed differences in peripheral and intrathecal immune cell profiles within the ALE cohort depending on the location of the target antigen. For this, the ALE cohort was subdivided into ALE patients with autoantibodies targeting extracellular antigens (ALE-Extra), intracellular antigens (ALE-Intra), and ALE patients without autoantibodies (AAB$^-$ ALE). UMAP analysis revealed comparable overall immune cell profiles between the three groups (Fig. 2A). Single parameters analysis identified higher percentages of PB lymphocytes in AAB$^-$ ALE compared to ALE-Extra while PB CD8$^+$ T cells were elevated in ALE-Intra in comparison to ALE-Extra (Fig. 2B, C, D). Significance of the latter was not maintained after correction for differences in age and sex. Regarding the CSF, AAB$^-$ ALE patients had increased percentages of T cells compared to ALE-Extra and ALE-Intra (Fig. 2B–E). In turn, ALE-Extra and ALE-Intra showed higher fractions of CSF B cells and plasma cells compared to AAB$^-$ ALE patients (Fig. 2B–F, G). Differences between ALE-Extra and AAB$^-$ ALE were confounded by age and sex. No significant differences in other PB or CSF immune cell populations were detected between ALE-Extra, ALE-Intra, and AAB$^-$ ALE (Supplementary Table 2).

In conclusion, intrathecal B and plasma cell responses are more pronounced in ALE patients with autoantibodies compared to AAB$^-$ ALE patients while the latter have higher percentages of lymphocytes in the PB and T cells in the CSF.

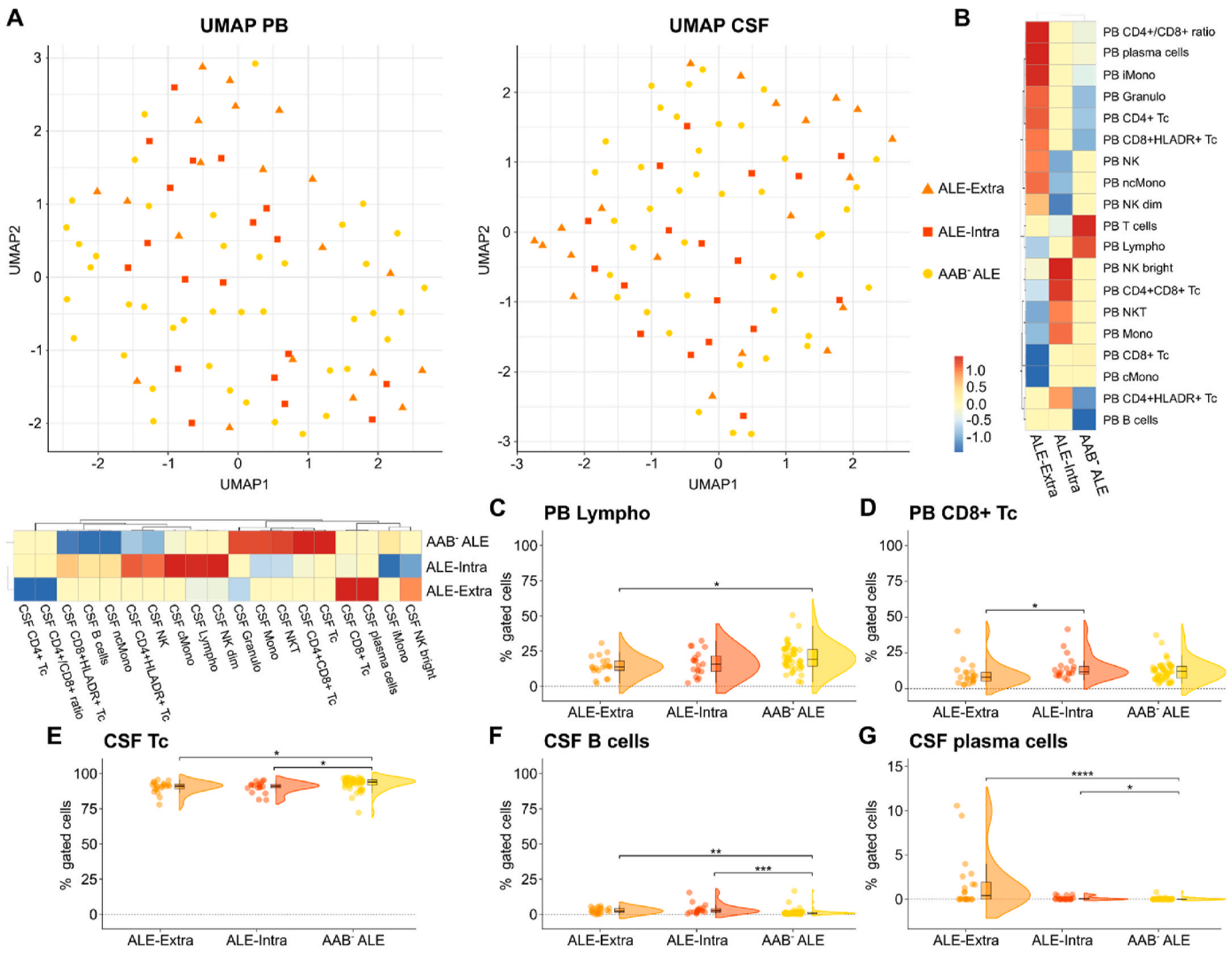

Fig. 2. Differences in PB and CSF immune cell profiles amongst ALE patients depending on the location of the target antigen.
A UMAP analysis including PB or CSF mFC parameters of ALE-Extra, ALE-Intra, and AAB$^-$ ALE patients. Each patient is shown as a multidimensional data point (triangle, square, or filled circle); **B** Heatmap analysis of PB or CSF mFC parameters: the median of each parameter was calculated, scaled, centered, and clustered hierarchically; **C-G** Violin plots with overlaying boxplots showing PB or CSF mFC parameters of ALE-Extra, ALE-Intra, and AAB$^-$ ALE patients. Boxes display the median as well as the 25th and 75th percentiles. The whiskers extend from the hinge to the largest and smallest values, respectively, but no further than 1.5 * IQR from the hinge. P-values were calculated by Kruskal Wallis test with Dunn post hoc test (p-adjustment method: Benjamini–Hochberg) as normality could not be assumed based on Shapiro–Wilk test. Only significant comparisons are illustrated.
AAB$^-$ - autoantibody-negative; ALE - autoimmune limbic encephalitis; ALE-Extra - ALE patients with autoantibodies targeting extracellular antigens; ALE-Intra - ALE patients with autoantibodies targeting intracellular antigens; *cMono - classical monocytes; CSF - cerebrospinal fluid; Granulo - granulocytes; iMono - intermediate monocytes; Lympho - lymphocytes; mFC - multidimensional flow cytometry; Mono - monocytes; ncMono - non-classical monocytes; NK - natural killer cells; NK bright - CD56^{bright} NK cells; NK dim - CD56^{dim} NK cells; NKT - natural killer T cells; PB - peripheral blood; Tc - T cells; UMAP - uniform manifold approximation and projection for dimension reduction.*
** p-value ≤ 0.05; ** p-value ≤ 0.01; *** p-value ≤ 0.001; **** p-value ≤ 0.0001.*

3.4. ALE and NMDARE show similarities in PB adaptive immunity with VME and diverge in innate immune cell patterns

As VME presents a relevant clinical differential diagnosis to AIE and can precede the development of AIE, we assessed the immune response of patients with VME at different time points (acute [aVME] and post-acute [pVME]) and compared it to the one seen in NMDARE, ALE, and SD patients. First, we focused on the PB immune response. The overall PB immune cell profile was comparable between groups as revealed by UMAP analysis (Fig. 3A).

Next, single parameters were analyzed in the PB of aVME, pVME, ALE, and NMDARE compared to SD controls (Fig. 3B–I).

With regard to the innate immune response, a shift from PB cMono to iMono was observed in aVME patients. IMono were also higher in pVME than in SD controls and ALE patients (Fig. 3B, C, D). PB granulocytes were elevated in ALE and NMDARE patients in comparison to SD controls (Fig. 3B–E).

Taking a closer look at the adaptive immune response, a decrease in the percentage of all PB lymphocytes was noted in ALE, NMDARE, aVME, and pVME patients (Fig. 3B–F). Differences between aVME and SD patients did not remain significant after correction for age and sex. In ALE patients, a shift from PB CD8$^+$ to CD4$^+$ T cells was observed (Fig. 3B–G-I). Activated CD4$^+$ and CD8$^+$ T cells were elevated in ALE, aVME, and pVME, but not in NMDARE patients compared to SD controls. Activated T cells were even higher in aVME/pVME than in ALE and NMDARE patients (Fig. 3B–J, K). Significance of differences between aVME/pVME and NMDARE were not maintained after correction for age and sex. Furthermore, PB plasma cells were increased in NMDARE,

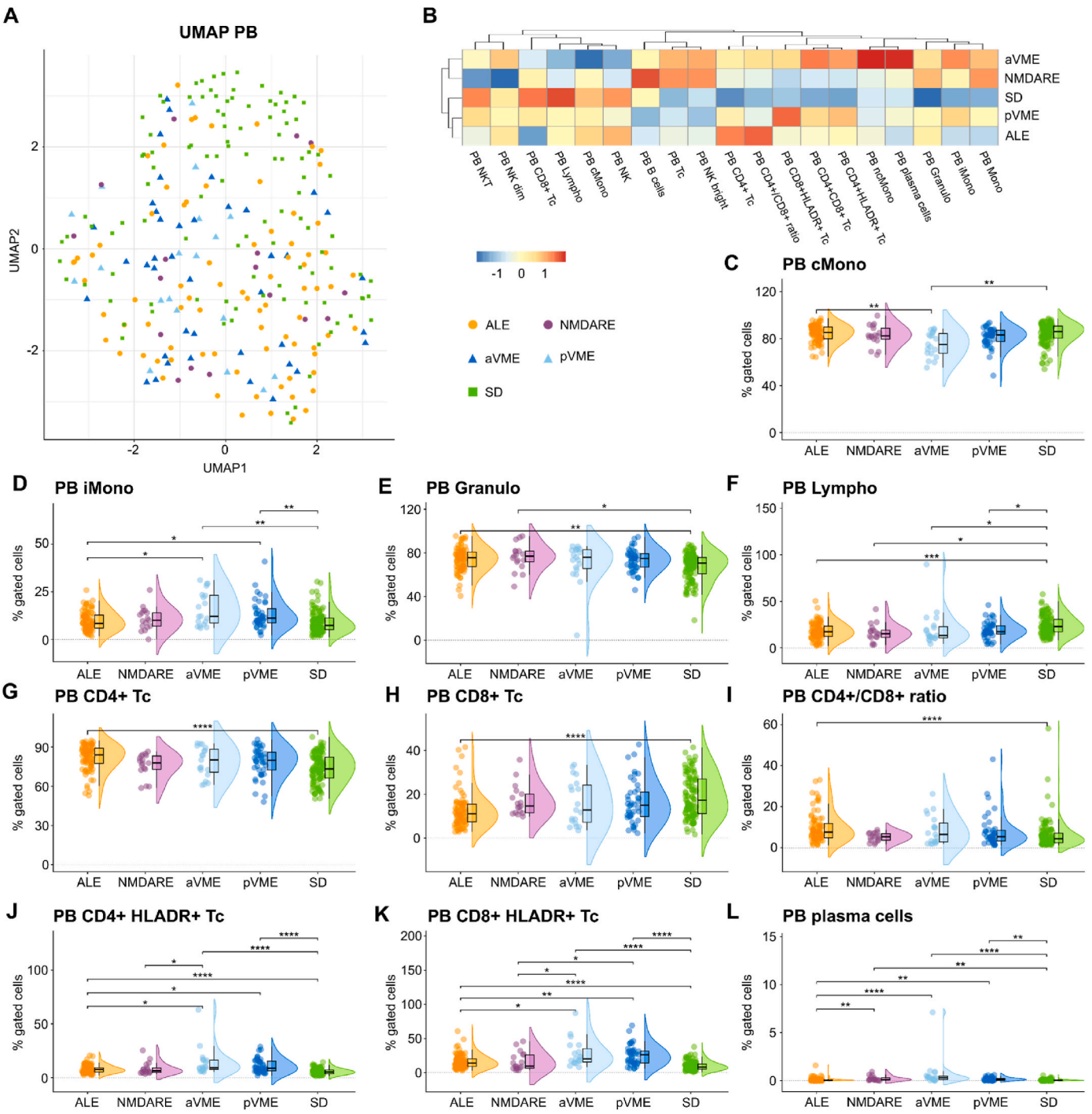

Fig. 3. Similarities in PB adaptive immune response and differences in innate immunity between ALE, NMDARE and VME.
A UMAP analysis including PB mFC parameters of ALE, NMDARE, a/pVME, and SD control patients. Each patient is shown as a multidimensional data point (triangle, square, or filled circle); **B** Heatmap analysis of PB mFC parameters: the median of each parameter was calculated, scaled, centered, and clustered hierarchically; **C-L** Violin plots with overlaying boxplots depicting the PB mFC parameters of ALE, NMDARE, a/pVME, and SD control patients. Boxes display the median as well as the 25th and 75th percentiles. The whiskers extend from the hinge to the largest and smallest values, respectively, but no further than 1.5 * IQR from the hinge. P-values were calculated by Kruskal Wallis test with Dunn post hoc test (p-adjustment method: Benjamini–Hochberg) as normality could not be assumed based on Shapiro–Wilk test. Only significant comparisons are illustrated.
ALE - autoimmune limbic encephalitis; aVME - acute viral meningoencephalitis; cMono - classical monocytes; CSF - cerebrospinal fluid; Granulo - granulocytes; iMono - intermediate monocytes; Lympho - lymphocytes; mFC - multidimensional flow cytometry; Mono - monocytes; ncMono - non-classical monocytes; NK - natural killer cells; NK bright - $CD56^{bright}$ NK cells; NK dim - $CD56^{dim}$ NK cells; NKT - natural killer T cells; NMDARE - anti-N-methyl-D-aspartate receptor encephalitis; PB - peripheral blood; pVME - post-acute viral meningoencephalitis; SD - somatic symptom disorder; Tc - T cells; UMAP - uniform manifold approximation and projection for dimension reduction; VME - viral meningoencephalitis.
** p-value ≤ 0.05; ** p-value ≤ 0.01; *** p-value ≤ 0.001; **** p-value ≤ 0.0001.*

aVME, and pVME patients compared to SD controls and ALE patients (Fig. 3B–L). The comparison between pVME and ALE was significantly confounded by age and sex differences.

As differences in PB lymphocytes and PB $CD8^+$ T cells were noted depending on the autoantibody status of ALE patients (Fig. 2B–D), we repeated the analyses for those parameters subdividing the ALE cohort into ALE-Extra, ALE-Intra, and AAB^- ALE. Reduced percentages of PB lymphocytes were only detected in ALE-Extra and ALE-Intra, not in AAB^- ALE in comparison to SD controls (Supplementary Fig. 1A). In turn, PB $CD8^+$ T cells were only reduced in ALE-Extra and AAB^- ALE, not in ALE-Intra in relation to SD controls (Supplementary Fig. 1B).

Taken together, VME patients show alterations in the PB monocyte compartment whereas ALE and NMDARE patients feature higher fractions of PB granulocytes compared to SD controls. ALE and VME patients share an increase in activated T cells whereas the shift from $CD8^+$ to $CD4^+$ T cells was only visible in ALE patients in comparison to SD controls. Activated T cells were even higher in VME than in ALE patients. NMDARE and VME patients both had an increase in PB plasma cells.

3.5. ALE, NMDARE, and VME patients share intrathecal T, B, and plasma cell responses while differentiating in NK cell patterns

We went on and repeated the analyses including CSF mFC parameters. UMAP analysis revealed a noticeable overlap between NMDARE and aVME/pVME patients while ALE patients clustered together with SD controls showing only a slight overlap with NMDARE and VME patients (Fig. 4A).

Next, single parameters were analyzed in the CSF of ALE, NMDARE, aVME, and pVME patients in relation to SD controls (Fig. 4B–M).

Focusing on the innate immune response, CSF monocytes and granulocytes were reduced in NMDARE, aVME, and pVME patients compared to SD controls and ALE patients (Fig. 4B–D). Differences in monocytes between ALE and NMDARE and in granulocytes between aVME and ALE, aVME and SD, and NMDARE and ALE were significantly confounded by age and sex. CSF NK cells, especially NK dim, were significantly higher in aVME and pVME patients compared to SD controls and ALE/NMDARE patients. Even higher fractions of NK cells were noted in aVME than in pVME patients (Fig. 4B–E, F). Significance in NK dim between aVME and NMDARE was not maintained after correction for age and sex. NK bright cells were reduced in NMDARE compared to ALE patients and SD controls as well as in aVME compared to ALE patients (Fig. 4B–G).

One pVME patient developed NMDARE at a later time point. As immune cell profiles between AIE and VME patients most markedly differed with regard to CSF NK cells, proportions of NK cells in PB and CSF of this patient were compared to the median of the other pVME patients and SD controls. Both PB NK and CSF NK were lower in that patient compared to the rest of the pVME cohort (median PB NK post-HSV NMDARE: 5.4 % vs other pVME 13.5 % vs SD 13.5 %; median CSF: post-HSV NMDARE: 2.3 % vs other pVME 3.5 %; SD 2.1 %) (Supplementary Figs. 1F and G). CSF NK dim were reduced while NK bright were increased in that patient compared to all other pVME patients (median CSF NK dim post-HSV NMDARE: 17.4 % vs other pVME 26.7 % vs SD 10.0 %; median CSF NK bright post-HSV NMDARE: 67.9 % vs other pVME 58.1 % vs SD 62.7 %) (Supplementary Fig. 1G).

Regarding the adaptive immune response, higher percentages of lymphocytes could be detected in the CSF of NMDARE, aVME, and pVME patients compared to SD controls and ALE patients (Fig. 4B–H). Differences between NMDARE and ALE were no longer significant after correction for age and sex. The overall fraction of CSF T cells was lower in NMDARE, aVME, and pVME patients compared to SD controls and ALE patients (Fig. 4B–I). Activated $CD4^+$ and $CD8^+$ T cells were increased in ALE, aVME, and pVME while only activated $CD8^+$ T cells were elevated in the CSF of NMDARE patients compared to SD controls. Activated $CD4^+$ T cells were even higher in aVME and pVME than in ALE and NMDARE patients (Fig. 4B–J, K). CSF B and plasma cells were increased in all patient groups in comparison to SD controls. CSF B cells were significantly higher in NMDARE and pVME compared to ALE patients and CSF plasma cells were increased in a/pVME compared to NMDARE and/or ALE patients (Fig. 4B–L, M). Differences in B cells between pVME and ALE as well as in plasma cells between a/pVME and ALE/NMDARE were no longer significant following correction for age and sex.

As differences in CSF T, B, and plasma cells were detected amongst ALE patients depending on the location of the target antigen (Fig. 2B–E-G), the analyses were repeated for those cell populations subdividing the ALE cohort into ALE-Extra, ALE-Intra, and AAB^- ALE. CSF T cells were only significantly higher in AAB^- ALE, not in ALE-Extra and ALE-Intra, compared to NMDARE, aVME, and pVME patients (Supplementary Fig. 1C). CSF B and plasma cells were elevated in ALE-Extra and ALE-Intra, but not in AAB^- ALE, in comparison to SD controls. CSF B and plasma cells were higher in ALE-Extra, ALE-Intra, NMDARE, aVME, and pVME compared to antibody-negative ALE. Furthermore, CSF plasma cells were also increased in a/pVME compared to ALE-Intra (Supplementary Figs. 1D and E).

Overall, ALE, NMDARE, and VME share an intrathecal increase in activated T cells. Antibody-positive ALE (especially with autoantibodies targeting extracellular antigens) and NMDARE patients also share a pronounced B and plasma cell response in the CSF with VME patients. Regarding innate immunity, NMDARE and VME are characterized by a reduction in CSF monocytes and granulocytes. VME patients feature an increase in CSF NK, especially NK dim, not visible in ALE or NMDARE patients. NK bright cells were reduced in NMDARE and aVME patients compared to SD controls and/or ALE patients.

3.6. MFC can support the diagnostic workup by differentiating AIE from similar clinical entities

As VME present an important clinical differential diagnoses to ALE and NMDARE, we were further interested in whether PB and CSF mFC could complement the diagnostic workup supporting early diagnosis and treatment. We therefore performed sPLS-DA in combination with ROC analysis to evaluate the performance of the PB mFC and/or CSF mFC and/or CSF routine parameters.

Using CSF routine in combination with PB/CSF mFC parameters as model input, ALE and aVME could be differentiated with an AUC of 0.995, CSF white blood cell count, CSF IgM, and CSF IgA being the three most important parameters (Fig. 5A). ALE and pVME could be differentiated with an AUC of 0.983, CSF white blood cell count, CSF lymphocytes, and CSF monocytes contributing the most to the model (Fig. 5B).

As AAB^- ALE is especially difficult to diagnose, we repeated the analyses only inlcuding this subgroup of ALE patients. AAB^- ALE and a/pVME patients could be differentiated with and AUC of 1.0, CSF white blood cell count, CSF IgM, and CSF IgA (AAB^-ALE vs aVME) and CSF lymphocytes, CSF monocytes, and CSF white blood cell count (AAB^-ALE vs pVME) being the most relevant parameters (Fig. 5C and D).

NMDARE and aVME could be differentiated with a perfect AUC (1.0), blood-CSF-barrier dysfunction, CSF white blood cell count, and CSF NK being the most important parameters of the model (Fig. 5E). NMDARE and pVME could be differentiated with an AUC of 0.979,with CSF white blood cell count, CSF lymphocytes, and blood-CSF-barrier dysfunction contributing the most to the model (Fig. 5F).

Finally, we combined ALE and NMDARE patients (AIE patients) and performed sPLS-DA analysis in comparison to aVME and pVME patients, respectively. AIE and aVME could be distinguished with an AUC of 0.993, CSF white blood cell count, CSF IgM, and CSF IgA presenting the most important parameters of the model (Fig. 5G). AIE and pVME could be differentiated with an AUC of 0.974, with CSF white blood cell count, CSF lymphocytes, and CSF monocytes being the most relevant parameters (Fig. 5H).

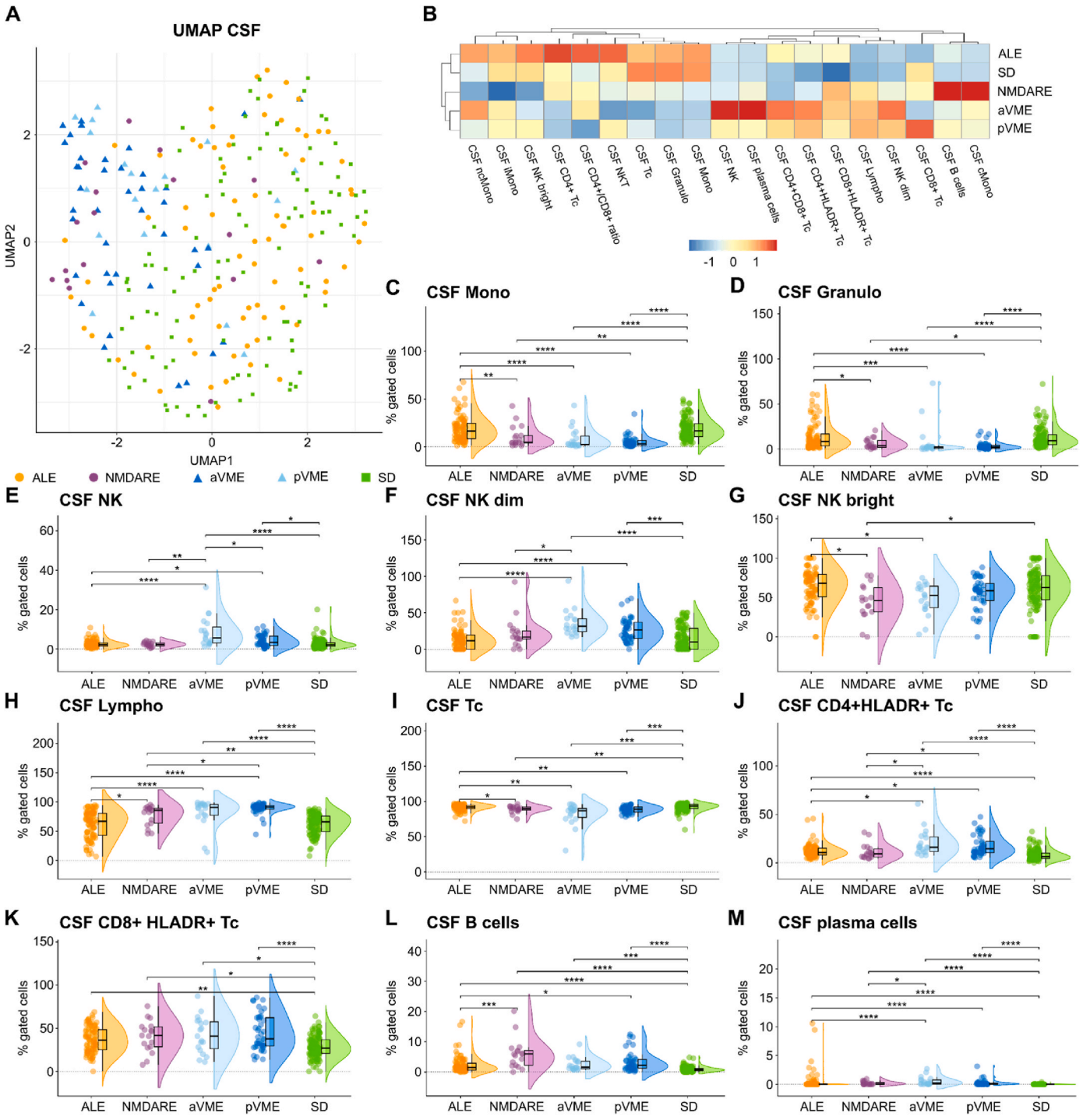

Fig. 4. ALE, NMDARE and VME share an intrathecal T, B, and plasma cell response while diverging in NK cell patterns.
A UMAP analysis including CSF mFC parameters of ALE, NMDARE, a/pVME, and SD control patients. Each patient is shown as a multidimensional data point (triangle, square, or filled circle); **B** Heatmap analysis of CSF mFC parameters: the median of each parameter was calculated, scaled, centered, and clustered hierarchically; **C-M** Violin plots with overlaying boxplots depicting the CSF mFC parameters of ALE, NMDARE, a/pVME, and SD control patients. Boxes display the median as well as the 25th and 75th percentiles. The whiskers extend from the hinge to the largest and smallest values, respectively, but no further than 1.5 * IQR from the hinge. P-values were calculated by Kruskal Wallis test with Dunn post hoc test (p-adjustment method: Benjamini–Hochberg) as normality could not be assumed based on Shapiro–Wilk test. Only significant comparisons are illustrated.
ALE - autoimmune limbic encephalitis; aVME - acute viral meningoencephalitis; Bc - B cell; cMono - classical monocytes; CSF - cerebrospinal fluid; Granulo - granulocytes; iMono - intermediate monocytes; Lympho - lymphocytes; mFC - multidimensional flow cytometry; Mono - monocytes; ncMono - non-classical monocytes; NK - natural killer cells; NK bright - CD56^{bright} NK cells; NK dim - CD56^{dim} NK cells; NKT - natural killer T cells; NMDARE - anti-N-methyl-D-aspartate receptor encephalitis; PB - peripheral blood; Pc - plasma cells; pVME - post-acute viral meningoencephalitis; SD - somatic symptom disorder; Tc - T cell(s); UMAP - uniform manifold approximation and projection for dimension reduction; VME - viral meningoencephalitis.
** p-value ≤ 0.05; ** p-value ≤ 0.01; *** p-value ≤ 0.001; **** p-value ≤ 0.0001.*

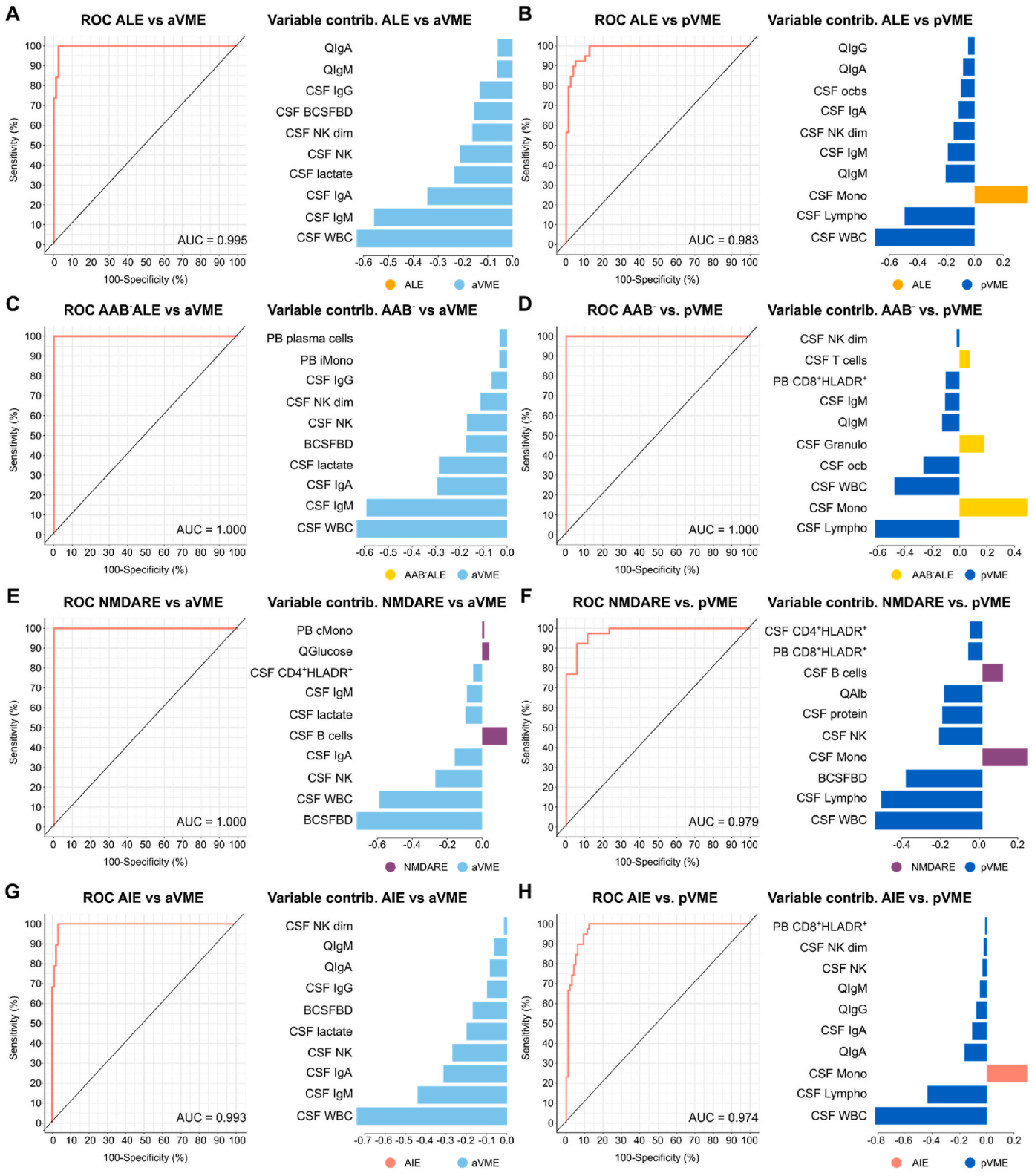

Fig. 5. MFC in combination with CSF routine parameters can perfectly differentiate ALE and NMDARE from VME patients.
A-H ROC analyses of the classification results obtained from sPLS-DA including CSF routine, PB and CSF mFC parameters. ALE patients (**A, B**), antibody-negative ALE patients (**C, D**), NMDARE patients (**E, F**), or AIE patients (ALE and NMDARE patients combined) (**G, H**) were compared to either aVME or pVME patients.
AAB⁻ALE - antibody-negative ALE; AIE - autoimmune encephalitis; ALE - autoimmune limbic encephalitis; AUC - Area under the curve; aVME - acute viral meningoencephalitis; BCSFBD - blood-CSF barrier dysfunction; cMono - classical monocytes; contrib. - contribution; CSF - cerebrospinal fluid; Granulo - granulocytes; iMono - intermediate monocytes; Lympho - lymphocytes; mFC - multidimensional flow cytometry; Mono - monocytes; NK - natural killer cells; NK bright - CD56^{bright} NK cells; NK dim - CD56^{dim} NK cells; NMDARE - anti-N-methyl-D-aspartate receptor encephalitis; ocb - oligoclonal bands; PB - peripheral blood; pVME - post-acute viral meningoencephalitis; Q - ratio; ROC - receiver operating characteristic; SD - somatic symptom disorder; sPLS-DA - Sparse Partial Least Squares Discriminant Analysis; WBC - white blood cell count.

Next, we repeated all analyses only including CSF routine parameters and found that using PB/CSF mFC parameters in combination with CSF routine parameters as model input was superior to CSF routine parameters alone (**Supplementare** Fig. 2A–H).

As lumbar puncture presents and invasive procedure and cannot be performed in all patients, we went on and assessed the discriminator ability of PB mFC parameters alone.

The models including PB mFC parameters were inferior to the models including PB/CSF mFC and/or CSF routine parameters. However, reasonable AUC values ranging from 0.778 to 0.894 were reached (Supplementary Figs. 2I–P).

In summary, the combination of CSF routine with PB/CSF mFC can perfectly discriminate ALE and NMDARE from aVME and pVME patients.

4. Discussion

AIE as a clinical entity became increasingly recognized over the last years and intensive efforts were made to characterize the pathophysiological mechanisms leading to a dysregulated immune response. Graus et al. suggested diagnostic criteria to enhance the diagnosis of AIE [5]. However, the diagnostic workup can be challenging in some cases causing therapeutic delay associated with poor outcomes [8,9]. Associations between viral infections and AIE have been described, the precise pathophysiological relevance and mechanisms remain insufficiently understood to date [24,25].

Previous studies analyzed immune cell patterns in CSF and brain parenchyma in subgroups of AIE patients and identified changes in the B and T cell response [14,16,17,20,36–41]. We performed a broad analysis of PB and CSF immune cell patterns in a sizable cohort of mainly treatment-naïve ALE and NMDARE patients and were able to confirm previously observed alterations in adaptive immunity in AIE. While NMDARE is mainly driven by a B and plasma cell response, ALE is characterized by a B and plasma cell as well as a pronounced T cell response. These changes are consistent with previous studies showing B and plasma cell accumulation in the CSF and brain parenchyma in NMDARE [38–41] and a B and plasma cell as well as T cell response in the CSF and brain parenchyma in ALE [14,16,17,20,36,37]. Thus, we were able to confirm previously described changes in adaptive immunity in a sizable mainly treatment-naïve cohort of NMDARE and ALE patients supporting the validity of our approach.

Viral infections, especially by herpes viruses, have been previously linked to the pathogenesis of AIE [24,25,42]. Around one third of HSVE patients develop AIE, mainly NMDARE, usually presenting within 3 months post HSVE [24]. However, the exact pathophysiological mechanisms contributing to AIE remain insufficiently understood to date.

A recently published study reported increased neutrophil counts and a higher monocyte-to-lymphocyte ratio in the PB of NMDARE patients in relation to VME and SD controls. In the CSF, T lymphocytes, especially $CD4^+$ lymphocytes were decreased in NMDARE compared to VME and higher percentages of $CD8^+$ T cells in PB and CSF correlated with disease severity of NMDARE [28]. Performing a broad characterization of innate and adaptive immune cell populations in well-defined cohorts of AIE and VME, we found similarities, mainly in the adaptive B and T cell-driven immune response between NMDARE, ALE, and VME. Even though there seem to be similarities in the overall adaptive immune response between AIE and VME, previous studies using single-cell RNA sequencing (sc-Seq) and single-cell B cell receptor sequencing (scBCR-seq) were able to identify differences in B cell subsets and functional phenotypes of B cells. NMDARE patients featured higher proportions of CSF IgD^-CD27^- double negative (DN) B cells and the B cells of these patients showed a more activated state compared to B cells from VME patients [43]. The interaction of B and T cells resulting in B cell expansion, generation of antibody-producing plasma cells and activation as well as clonal expansion of T cells has been reported to be critically involved in the pathogenesis of CNS autoimmune diseases [44,45]. In this context, complex formation between foreign- and self-antigens can lead to T cells specific to foreign antigens providing help to autoreactive B cells [44]. Taken together, further studies performing an in-depth immune cell and repertoire profiling will be necessary to assess the contribution of viral triggers to the pathogenesis of AIE.

Main differences between the immune cell profile of VME and AIE were seen with regard to the innate immune response, predominantly the NK cell compartment. NK cells are known to be important mediators of the anti-viral immune response which could account for higher proportions of NK cells in VME compared to AIE [46,47]. In our cohort, VME patients showed an intrathecal increase in NK cells, especially NK dim. NK dim are reported to possess a high cytotoxic capacity contributing to the anti-viral and anti-tumor immune response [48]. In contrast, NK bright cells are very efficient in cytokine production. They release interferon- γ, granulocyte–macrophage colony-stimulating factor, tumor necrosis factor-α, IL-10, and IL-13, depending on the activating conditions. Furthermore, NK bright cells possess immunoregulatory functions [48]. Regulatory NK cells are able to limit the development of autoantibody-secreting B cells [49] and contribute to the inhibition of autoreactive T cells [50–52]. In line with that, we detected lower percentages of NK bright cells in the CSF of our NMDARE cohort compared to SD controls. It is intriguing to speculate that an impaired NK cell response might contribute to the excessive and prolonged B cell, plasma cell, and T cell response seen in AIE. The potential role of NK cells in the pathogenesis of AIE is supported by lower proportions of CSF and PB NK cells post-VME in the patient who developed NMDARE later on compared to the median of the other pVME patients. A shift from CSF NK dim to CSF NK bright in this patient may suggest a reduction in cytotoxic activity and an increase in immunoregulatory capacities. Unfortunately, due to the difficulty of obtaining these longitudinal samples, data was only available for one patient. On a functional level, previous studies found a dysregulation of regulatory $CD56^{bright}$ NK cells, with a reduced ability to inhibit autologous T cell proliferation, contributing to CNS autoimmune diseases, e.g. multiple sclerosis (MS) [53]. Another study reported an impaired control of autoimmunity by NKG2C + NK cells. In addition, EBV-variant (Latent membrane protein 1 (LMP-1) peptide)-specific upregulation of the immunomodulatory HLA-E has been described to facilitate immune evasion by preventing the killing of autoreactive T cells by NKG2A + cells contributing to the development of MS [54]. Thus, further studies on the exact phenotype and functions of NK cells might yield relevant insights into the pathogenesis of AIE and might contribute to the identification of novel treatment targets.

Apart from differences in NK cells, changes in monocyte populations were detected in the PB and CSF of AIE and VME patients. Monocytes are differentiated into three main subpopulations based on their expression of CD14 and CD16 (cMono: $CD14^{hi}$CD16-, ncMono: $CD14^{low}CD16^{high}$, and iMono: CD14+CD16+). NcMono have been reported to possess a more anti-inflammatory phenotype, while cMono and iMono are regarded to be more pro-inflammatory [55,56]. Monocytes have been previously detected to be crucially involved in the pathogenesis of CNS viral infections and CNS autoimmune disorders. In the case of viral encephalitis, infiltration of monocytes in the inflamed tissue and their contribution to the local inflammation, e.g. by differentiation into inflammatory macrophages, secretion of pro-inflammatory cytokines, and disruption of blood-brain-barrier integrity, has been described [56,57]. In CNS autoimmune disorders like multiple sclerosis, shifts in peripheral, intrathecal, and intraparenchymal monocyte populations have been observed and monocytes were found to contribute to acute inflammation, activation of autoreactive T cells via differentiation to dendritic cells, demyelination, and tissue destruction [56,58]. The pathophysiological relevance of infiltrating monocytes in viral CNS infections as well as in CNS autoimmune disorders is further emphasized by the fact that reduction in local monocyte infiltration mitigates the disease course [59]. In the current study, we found reduced amounts of monocytes in the CSF of NMDARE and VME patients, which might

indicate invasion into the brain parenchyma to the site of inflammation, where monocytes are involved in the local pathology. In the PB, VME patients featured a shift from cMono to iMono. Given the different phenotypical and functional states of myeloid cells as well as their pathophysiological relevance in CNS infections and autoimmune diseases, an in-depth characterization of monocyte subsets might be promising to improve the pathophysiological understanding of these disease entities and to identify novel treatment approaches.

Beyond the pathophysiological mechanism, we were interested in the clinical approach of AIE.

Diagnosis of AIE can be challenging, especially if antibody testing yields negative results. However, early diagnosis and therapy are crucial as treatment delay is associated with permanent neurologic deficits and a worse prognosis [8,9]. AVME and pVME present entities which can be confused with AIE based on clinical and radiological features [60,61]. We therefore assessed whether mFC could be a useful tool to distinguish AIE from clinical differential diagnoses supporting the diagnosis of AIE. Our results indicate that PB/CSF mFC in combination with CSF routine analysis can perfectly discriminate between VME, (antibody-negative) ALE, and NMDARE. The combination of mFC with CSF routine analysis was superior to CSF routine analysis alone. Furthermore, PB mFC combined with novel computational approaches might be a beneficial non-invasive approach supporting the diagnosis in patients who are not eligible for a lumbar puncture.

Taken together, our data prove that mFC of PB and CSF might be a useful tool in the diagnostic workup of AIE, presenting a valuable complement to the established diagnostic approach promoting early diagnosis and treatment to improve outcomes.

Our study is limited by the retrospective design, the lack of an independent validation cohort as well as differences in age and sex between groups. Furthermore, samples were not analyzed at the same time point as mFC data were acquired during clinical routine workup. 20.4 % of AIE patients were pretreated with immunotherapy or plasmapheresis. As the time frame between the last treatment and the mFC analysis was not available, we cannot rule out treatment-effects on immune cell profiles in these cases. As the scope of the current study was to analyze the peripheral and intrathecal immune cell profiles of ALE, NMDARE, and VME patients compared to SD controls and to assess the diagnostic potential, MRI data were not analyzed as part of the study. Correlating immune cell changes in the PB and CSF with MRI abnormalities could support the pathophysiological relevance of certain immune cell subsets, which would be an interesting topic for future studies. Furthermore, disease duration was not available for the ALE and NMDARE cohorts. However, peripheral and intrathecal immune cell profiles can vary depending on the disease stage. Thus, future studies should include the duration of the disease and assess changes of PB and CSF immune cell profiles depending on the stage of the disease. Moreover, it has to been acknowledged that antibody-negative ALE patients might have unknown antibodies or antibodies not detectable by the assays used.

Regarding the viral encephalitis cohort, only patients with herpes viruses were included in the study. However, several other viruses can cause encephalitis (e.g., tick-borne encephalitis virus, west nile virus, enteroviruses, and adenoviruses). The peripheral and intrathecal immune mechanisms can vary depending on the underlying type of virus. Thus, our findings might not be applicable to other CNS viral infections. Analyzing the immune response in other forms of CNS viral infections and comparing them with autoimmune encephalitis might be an interesting topic for future studies. Given the wide availability of herpes virus PCR testing, the diagnosis can be confirmed quickly. However, PB mFC may be useful in patients who are not eligible for lumbar puncture. Furthermore, mFC might support the diagnosis early during the disease course, when the PCR can be negative in some cases [62,63]. Once mFC is established at a department, it can be performed easily with the results being available on the same day. Further studies should clarify the benefit of mFC in the diagnostic workup of viral encephalitis including patients with viral encephalitis caused by other (non-herpes) viruses as these can present a diagnostic challenge.

Despite the limitations, our study exceeds previous studies in several ways: 1. We analyzed the PB and CSF immune cell profile from a sizable, well-defined cohort of mainly immunotherapy-naïve AIE patients compared to SD controls and clinical differential diagnoses. 2. We combined mFC with novel computational approaches facilitating the identification of possible pathophysiological mechanisms of AIE with implications on diagnosis and treatment to improve outcomes.

5. Conclusion

In summary, our results point towards a relevant involvement of the adaptive immune system in the pathophysiology of AIE and a contribution of the NK cell compartment to the pathogenesis of autoimmunity. Above that, our data suggests that mFC could be a valuable complement to the diagnostic workup of AIE under certain circumstances facilitating early diagnosis and initiation of appropriate therapy to improve patients' outcomes.

CRediT authorship contribution statement

Saskia Räuber: Writing – review & editing, Writing – original draft, Visualization, Methodology, Investigation, Funding acquisition, Formal analysis, Data curation, Conceptualization. **Andreas Schulte-Mecklenbeck:** Writing – review & editing, Investigation, Formal analysis, Data curation. **Kelvin Sarink:** Software, Methodology, Formal analysis. **Kristin S. Golombeck:** Investigation. **Christina B. Schroeter:** Writing – review & editing, Investigation. **Alice Willison:** Writing – review & editing. **Christopher Nelke:** Investigation. **Christine Strippel:** Writing – review & editing, Investigation. **Andre Dik:** Investigation. **Marco Gallus:** Investigation. **Stjepana Kovac:** Writing – review & editing. **Heinz Wiendl:** Resources. **Gerd Meyer zu Hörste:** Resources. **Tobias Ruck:** Resources. **Oliver M. Grauer:** Investigation. **Udo Dannlowski:** Supervision, Resources. **Tim Hahn:** Supervision, Resources. **Catharina C. Gross:** Supervision, Resources, Project administration. **Sven G. Meuth:** Supervision, Resources, Project administration, Funding acquisition. **Nico Melzer:** Writing – review & editing, Supervision, Resources, Project administration, Funding acquisition, Conceptualization.

Data sharing

Further information and requests for resources, anonymized clinical and flow cytometry data should be directed to and will be fulfilled by **Nico Melzer** (Nico.Melzer@med.uni-duesseldorf.de).

Funding

This work was supported by the German Federal Ministry of Education and Research (Comprehensive, Orchestrated, National Network to Explain, Categorize and Treat autoimmune encephalitis and allied diseases within the German NEtwork for Research on AuToimmune Encephalitis – CONNECT GENERATE; 01GM1908), the Research Committee of the Faculty of Medicine of the Heinrich Heine University Düsseldorf (grant number 2022–04), and by the IMF (Innovative Medizinische Forschung), grant to SK (KO122003).

10. List of abbreviations

Abbreviation	Explanation
AABs	autoantibodies
ADEM	acute disseminated encephalomyelitis
AIE	autoimmune encephalitis
ALE	autoimmune limbic encephalitis
AUC	area under the curve
aVME	acute viral meningoencephalitis
BCSFBD	blood-CSF-barrier dysfunction

(*continued on next page*)

(*continued*)

CASPR2	contactin-associated protein-like 2
cMono	classical monocytes
CNS	central nervous system
CSF	cerebrospinal fluid
DPPX	dipeptidyl-peptidase–like protein 6
EBV	Epstein-Barr virus
EEG	electroencephalography
GABA-A-R	γ-aminobutyric acid A receptor
GABA-B-R	γ-aminobutyric acid B receptor
GAD65	65 kDa isoform of the glutamic acid decarboxylase
GFAP	glial fibrillary acidic protein
GluRD2	glutamate receptor δ2
Granulo	granulocytes
HLA	human leukocyte antigen
HSV	herpes simplex virus 1/2
Ig	immunoglobulin
IgLON5	IgLON family member 5
iMono	intermediate monocytes
ITPR1	Inositol 1,4,5-trisphosphate receptor type 1
LGI1	leucine-rich, glioma inactivated 1
Lympho	lymphocytes
mFC	multidimensional flow cytometry
mGluR1	Metabotropic glutamate receptor 1
mGluR5	Metabotropic glutamate receptor 5
MOG	Myelin oligodendrocyte glycoprotein
Mono	monocytes
MRI	magnetic resonance imaging
ncMono	non-classical monocytes
NK	natural killer cells
NK bright	$CD56^{bright}$ NK cells
NK dim	$CD56^{dim}$ NK cells
NKT	natural killer T cells
NMDAR	N-methyl-D-aspartate receptor
NMDARE	anti-NMDAR encephalitis
ocbs	oligoclonal bands
PB	peripheral blood
PCR	polymerase chain reaction
pVME	post-acute viral meningoencephalitis
ROC	receiver operating characteristic
sPLS-DA	Sparse Partial Least Squares Discriminant Analysis
UMAP	uniform manifold approximation and projection for dimension reduction
VGKC	voltage-gated potassium channel
VME	viral meningoencephalitis
VZV	varicella-zoster virus
WBC	white blood cell count
Zic4	Zinc finger protein 4

Declaration of competing interest

SK reports research funding from Biogen and has received speakers' honoraria from Eisai, Jazz Pharma and UCB. The remaining authors report no conflicts of interest.

Acknowledgments

We thank the Core Facility Flow Cytometry at the Medical Faculty of the Heinrich-Heine University Düsseldorf, Germany for assistance in sample analysis. Moreover, we would like to thank all participating patients and their relatives and caregivers for their invaluable contribution to this study.

Appendix A. Supplementary data

Supplementary data to this article can be found online at https://doi.org/10.1016/j.jaut.2025.103396.

References

[1] N. Melzer, T. Budde, O. Stork, S.G. Meuth, Limbic encephalitis: potential impact of adaptive autoimmune inflammation on neuronal circuits of the amygdala, Front. Neurol. 6 (171) (2015).

[2] J. Dalmau, F. Graus, Antibody-mediated encephalitis, N. Engl. J. Med. 378 (9) (2018) 840–851.

[3] J. Granerod, H.E. Ambrose, N.W.S. Davies, J.P. Clewley, A.L. Walsh, D. Morgan, et al., Causes of encephalitis and differences in their clinical presentations in England: a multicentre, population-based prospective study, Lancet Infect. Dis. 10 (12) (2010) 835–844.

[4] D. Dubey, S.J. Pittock, C.R. Kelly, A. McKeon, A.S. Lopez-Chiriboga, V.A. Lennon, et al., Autoimmune encephalitis epidemiology and a comparison to infectious encephalitis, Ann. Neurol. 83 (1) (2018) 166–177.

[5] F. Graus, M.J. Titulaer, R. Balu, S. Benseler, C.G. Bien, T. Cellucci, et al., A clinical approach to diagnosis of autoimmune encephalitis, Lancet Neurol. 15 (4) (2016) 391–404.

[6] M.S. Gable, H. Sheriff, J. Dalmau, D.H. Tilley, C.A. Glaser, The frequency of autoimmune N-methyl-D-aspartate receptor encephalitis surpasses that of individual viral etiologies in young individuals enrolled in the California Encephalitis Project, Clin. Infect. Dis. 54 (7) (2012) 899–904.

[7] T. Cellucci, H. Van Mater, F. Graus, E. Muscal, W. Gallentine, M.S. Klein-Gitelman, et al., Clinical approach to the diagnosis of autoimmune encephalitis in the pediatric patient, Neurology - Neuroimmunology Neuroinflammation 7 (2) (2020) e663.

[8] E.H. Breese, J. Dalmau, V.A. Lennon, M. Apiwattanakul, D.K. Sokol, Anti-N-methyl-D-aspartate receptor encephalitis: early treatment is beneficial, Pediatr. Neurol. 42 (3) (2010) 213–214.

[9] S. Byrne, C. Walsh, Y. Hacohen, E. Muscal, J. Jankovic, A. Stocco, et al., Earlier treatment of NMDAR antibody encephalitis in children results in a better outcome, Neurol Neuroimmunol Neuroinflamm 2 (4) (2015) e130.

[10] C. Pantoja-Ruiz, C. Santucci, L. Arenas, L. Casallas, G. Castellanos, Autoimmune encephalitis: what has changed during the past 15 years? Clinical and Experimental Neuroimmunology 10 (4) (2019) 291–300.

[11] A. Vincent, C.G. Bien, S.R. Irani, P. Waters, Autoantibodies associated with diseases of the CNS: new developments and future challenges, Lancet Neurol. 10 (8) (2011) 759–772.

[12] E. Lancaster, J. Dalmau, Neuronal autoantigens–pathogenesis, associated disorders and antibody testing, Nat. Rev. Neurol. 8 (7) (2012) 380–390.

[13] N. Melzer, S.G. Meuth, H. Wiendl, Neuron-directed autoimmunity in the central nervous system: entities, mechanisms, diagnostic clues, and therapeutic options, Curr. Opin. Neurol. 25 (3) (2012) 341–348.

[14] C.G. Bien, A. Vincent, M.H. Barnett, A.J. Becker, I. Blümcke, F. Graus, et al., Immunopathology of autoantibody-associated encephalitides: clues for pathogenesis, Brain 135 (5) (2012) 1622–1638.

[15] S.J. Crisp, D.M. Kullmann, A. Vincent, Autoimmune synaptopathies, Nat. Rev. Neurosci. 17 (2) (2016) 103–117.

[16] K.S. Golombeck, K. Bönte, C. Mönig, K.M. van Loo, M. Hartwig, W. Schwindt, et al., Evidence of a pathogenic role for CD8+ T cells in anti-GABAB receptor limbic encephalitis, Neurology - Neuroimmunology Neuroinflammation 3 (3) (2016) e232.

[17] A. Bracher, C. Alcalá, J. Ferrer, N. Melzer, R. Hohlfeld, B. Casanova, et al., An expanded parenchymal CD8+ T cell clone in GABA(A) receptor encephalitis, Ann Clin Transl Neurol 7 (2) (2020) 239–244.

[18] C. Geis, A. Weishaupt, S. Hallermann, B. Grünewald, C. Wessig, T. Wultsch, et al., Stiff person syndrome-associated autoantibodies to amphiphysin mediate reduced GABAergic inhibition, Brain 133 (11) (2010) 3166–3180.

[19] J. Pitsch, D. Kamalizade, A. Braun, J.C. Kuehn, P.E. Gulakova, T. Rüber, et al., Drebrin autoantibodies in patients with seizures and suspected encephalitis, Ann. Neurol. 87 (6) (2020) 869–884.

[20] F. Bernal, F. Graus, À. Pifarré, A. Saiz, B. Benyahia, T. Ribalta, Immunohistochemical analysis of anti-Hu-associated paraneoplastic encephalomyelitis, Acta Neuropathol. 103 (5) (2002) 509–515.

[21] N. Melzer, S.G. Meuth, H. Wiendl, CD8+ T cells and neuronal damage: direct and collateral mechanisms of cytotoxicity and impaired electrical excitability, FASEB J. 23 (11) (2009) 3659–3673.

[22] S. Muñiz-Castrillo, A. Vogrig, J. Honnorat, Associations between HLA and autoimmune neurological diseases with autoantibodies, Auto Immun Highlights 11 (1) (2020) 2.

[23] A. Vogrig, S. Muñiz-Castrillo, V. Desestret, B. Joubert, J. Honnorat, Pathophysiology of paraneoplastic and autoimmune encephalitis: genes, infections, and checkpoint inhibitors, Ther Adv Neurol Disord 13 (2020) 1756286420932797.

[24] T. Armangue, M. Spatola, A. Vlagea, S. Mattozzi, M. Cárceles-Cordon, E. Martinez-Heras, et al., Frequency, symptoms, risk factors, and outcomes of autoimmune encephalitis after herpes simplex encephalitis: a prospective observational study and retrospective analysis, Lancet Neurol. 17 (9) (2018) 760–772.

[25] F. Graus, A. Saiz, J. Dalmau, Antibodies and neuronal autoimmune disorders of the CNS, J. Neurol. 257 (4) (2010) 509–517.

[26] zu Hörste G. Meyer, C.C. Gross, L. Klotz, N. Schwab, H. Wiendl, Next-generation neuroimmunology: new technologies to understand central nervous system autoimmunity, Trends Immunol. 41 (4) (2020) 341–354.

[27] C.C. Gross, A. Schulte-Mecklenbeck, L. Madireddy, M. Pawlitzki, C. Strippel, S. Räuber, et al., Classification of neurological diseases using multi-dimensional cerebrospinal fluid analysis, Brain 144 (9) (2021) 2625–2634.

[28] J. Wang, L. Luo, Z. Meng, Y. Ren, M. Tang, Z. Huang, et al., Blood and CSF findings of cellular immunity in anti-NMDAR encephalitis, Int. Immunopharmacol. 130 (2024) 111743.

[29] World Health Organization. Schizophrenia, schizotypal and delusional disorders. International Statistical Classification of Disease and Related Health Problems. Tenth Revision. Version:2019. [Internet]. [cited 2021 Mar 27]. Available from: https://icd.who.int/browse10/2019/en#/F40-F48.

[30] C.J. Buck, ICD-10-CM Standard Edition, E-Book, Elsevier Health Sciences, 2018, 2017.
[31] G. Lueg, C.C. Gross, H. Lohmann, A. Johnen, A. Kemmling, M. Deppe, et al., Clinical relevance of specific T-cell activation in the blood and cerebrospinal fluid of patients with mild Alzheimer's disease, Neurobiol. Aging 36 (1) (2015) 81–89.
[32] S. Räuber, M. Heming, J. Repple, T. Ruland, R. Kuelby, A. Schulte-Mecklenbeck, et al., Cerebrospinal fluid flow cytometry distinguishes psychosis spectrum disorders from differential diagnoses, Mol Psychiatry 26 (12) (2021) 7661–7670.
[33] S. Räuber, A. Schulte-Mecklenbeck, A. Willison, R. Hagler, M. Jonas, D. Pul, et al., Flow cytometry identifies changes in peripheral and intrathecal lymphocyte patterns in CNS autoimmune disorders and primary CNS malignancies, J. Neuroinflammation 21 (1) (2024) 286.
[34] H. Reiber, J.B. Peter, Cerebrospinal fluid analysis: disease-related data patterns and evaluation programs, J. Neurol. Sci. 184 (2) (2001) 101–122.
[35] C.C. Gross, A. Schulte-Mecklenbeck, A. Rünzi, T. Kuhlmann, A. Posevitz-Fejfár, N. Schwab, et al., Impaired NK-mediated regulation of T-cell activity in multiple sclerosis is reconstituted by IL-2 receptor modulation, Proc. Natl. Acad. Sci. USA 113 (21) (2016) E2973–E2982.
[36] N. Hansen, K. Schwing, D. Önder, G. Widman, P. Leelaarporn, I. Prusseit, et al., Low CSF CD4/CD8 + T-cell proportions are associated with blood–CSF barrier dysfunction in limbic encephalitis, Epilepsy Behav. 102 (2020).
[37] N. Hansen, D. Önder, K. Schwing, G. Widman, P. Leelaarporn, I. Prusseit, et al., CD19+ B-cells in autoantibody-negative limbic encephalitis, Epilepsy Behav. 106 (2020) 107016.
[38] J.-P. Camdessanché, N. Streichenberger, G. Cavillon, V. Rogemond, G. Jousserand, J. Honnorat, et al., Brain immunohistopathological study in a patient with anti-NMDAR encephalitis, Eur. J. Neurol. 18 (6) (2011) 929–931.
[39] R.C. Dale, S. Pillai, F. Brilot, Cerebrospinal fluid CD19+ B-cell expansion in N-methyl-D-aspartaze receptor encephalitis, Dev. Med. Child Neurol. 55 (2) (2013) 191–193.
[40] E. Martinez-Hernandez, J. Horvath, Y. Shiloh-Malawsky, N. Sangha, M. Martinez-Lage, J. Dalmau, Analysis of complement and plasma cells in the brain of patients with anti-NMDAR encephalitis, Neurology 77 (6) (2011) 589–593.
[41] I. Wagnon, P. Hélie, I. Bardou, C. Regnauld, L. Lesec, J. Leprince, et al., Autoimmune encephalitis mediated by B-cell response against N-methyl-d-aspartate receptor, Brain 143 (10) (2020) 2957–2972.
[42] J. Dalmau, M.R. Rosenfeld, Paraneoplastic syndromes of the CNS, Lancet Neurol. 7 (4) (2008) 327–340.
[43] S. Li, X. Hu, M. Wang, L. Yu, Q. Zhang, J. Xiao, et al., Single-cell RNA sequencing reveals diverse B cell phenotypes in patients with anti-NMDAR encephalitis, Psychiatr. Clin. Neurosci. 78 (3) (2024) 197–208.
[44] R. Iversen, L.M. Sollid, Dissecting autoimmune encephalitis through the lens of intrathecal B cells, Proc. Natl. Acad. Sci. USA 121 (9) (2024) e2401337121.
[45] J. Theorell, R. Harrison, R. Williams, M.I.J. Raybould, M. Zhao, H. Fox, et al., Ultrahigh frequencies of peripherally matured LGI1- and CASPR2-reactive B cells characterize the cerebrospinal fluid in autoimmune encephalitis, Proceedings of the National Academy of Sciences of the United States of America 121 (7) (2024) e2311049121.
[46] Christine A. Biron, Khuong B. Nguyen, Gary C. Pien, P. Leslie, a Cousens, T. P. Salazar-Mather, Natural killer cells in antiviral defense: function and regulation by innate cytokines, Annu. Rev. Immunol. 17 (1) (1999) 189–220.
[47] A.R. French, W.M. Yokoyama, Natural killer cells and autoimmunity, Arthritis Res. Ther. 6 (1) (2003) 8.
[48] A. Poli, T. Michel, M. Thérésine, E. Andrès, F. Hentges, J. Zimmer, CD56bright natural killer (NK) cells: an important NK cell subset, Immunology 126 (4) (2009) 458–465.
[49] K. Takeda, G. Dennert, The development of autoimmunity in C57BL/6 lpr mice correlates with the disappearance of natural killer type 1-positive cells: evidence for their suppressive action on bone marrow stem cell proliferation, B cell immunoglobulin secretion, and autoimmune symptoms, The Journal of experimental medicine 177 (1) (1993) 155–164.
[50] R.B. Smeltz, N.A. Wolf, R.H. Swanborg, Inhibition of autoimmune T cell responses in the DA rat by bone marrow-derived NK cells in vitro: implications for autoimmunity, Journal of immunology (Baltimore, Md : 1950) 163 (3) (1999) 1390–1397.
[51] B. Bielekova, M. Catalfamo, S. Reichert-Scrivner, A. Packer, M. Cerna, T. A. Waldmann, et al., Regulatory CD56(bright) natural killer cells mediate immunomodulatory effects of IL-2Ralpha-targeted therapy (daclizumab) in multiple sclerosis, Proceedings of the National Academy of Sciences of the United States of America 103 (15) (2006) 5941–5946.
[52] W. Jiang, N.R. Chai, D. Maric, B. Bielekova, Unexpected role for granzyme K in CD56bright NK cell-mediated immunoregulation of multiple sclerosis, J. Immunol. 187 (2) (2011) 781–790.
[53] A. Laroni, E. Armentani, N. Kerlero de Rosbo, F. Ivaldi, E. Marcenaro, S. Sivori, et al., Dysregulation of regulatory CD56bright NK cells/T cells interactions in multiple sclerosis, J. Autoimmun. 72 (2016) 8–18.
[54] H. Vietzen, S.M. Berger, L.M. Kühner, P.L. Furlano, G. Bsteh, T. Berger, et al., Ineffective control of Epstein-Barr-virus-induced autoimmunity increases the risk for multiple sclerosis, Cell 186 (26) (2023) 5705, 18.e13.
[55] P.B. Narasimhan, P. Marcovecchio, A.A.J. Hamers, C.C. Hedrick, Nonclassical monocytes in health and disease, Annu. Rev. Immunol. 37 (2019) 439–456.
[56] T.M. Ashhurst, C. van Vreden, P. Niewold, N.J. King, The plasticity of inflammatory monocyte responses to the inflamed central nervous system, Cell. Immunol. 291 (1–2) (2014) 49–57.
[57] A. Waschbisch, S. Schröder, D. Schraudner, L. Sammet, B. Weksler, A. Melms, et al., Pivotal role for CD16+ monocytes in immune surveillance of the central nervous system, J. Immunol. 196 (4) (2016) 1558–1567.
[58] M. Carstensen, T. Christensen, M. Stilund, H.J. Møller, E.L. Petersen, T. Petersen, Activated monocytes and markers of inflammation in newly diagnosed multiple sclerosis, Immunol. Cell Biol. 98 (7) (2020) 549–562.
[59] D.R. Getts, R.L. Terry, M.T. Getts, C. Deffrasnes, M. Müller, C. van Vreden, et al., Therapeutic inflammatory monocyte modulation using immune-modifying microparticles, Sci. Transl. Med. 6 (219) (2014) 219ra7.
[60] T. Armangue, F. Leypoldt, J. Dalmau, Autoimmune encephalitis as differential diagnosis of infectious encephalitis, Curr. Opin. Neurol. 27 (3) (2014) 361–368.
[61] A.J. da Rocha, R.H. Nunes, A.C.M. Maia, L.L.F. do Amaral, Recognizing autoimmune-mediated encephalitis in the differential diagnosis of limbic disorders, Am. J. Neuroradiol. 36 (12) (2015) 2196–2205.
[62] J.I. Roberts, G.A.E. Jewett, R. Tellier, P. Couillard, S. Peters, Twice negative PCR in a patient with herpes simplex virus type 1 (HSV-1) encephalitis, Neurohospitalist 11 (1) (2021) 66–70.
[63] X. De Tiège, B. Héron, P. Lebon, G. Ponsot, F. Rozenberg, Limits of early diagnosis of herpes simplex encephalitis in children: a retrospective study of 38 cases, Clin. Infect. Dis. 36 (10) (2003) 1335–1339.